

Collapse behaviour in reciprocal frame structures

Elsa Garavaglia^{1a}, Attilio Pizzigoni^{2b}, Luca Sgambi^{*1} and Noemi Basso^{1c}

¹Department of Civil and Environmental Engineering, Politecnico di Milano, Milan, Italy

²Department of Design and Technology, Università degli Studi di Bergamo, Bergamo, Italy

(Received September 7, 2012, Revised March 4, 2013, Accepted April 25, 2013)

Abstract. “Reciprocal Frame” refers to a self-supporting grid structure used both for floor and roof. Using Finite Element Methods for non-linear solid mechanics and frictional-contact, this paper intends to analytically and numerically investigate the collapse behaviour of a reciprocal frame structure made of fibre-reinforced concrete. Considering a simple 3-beam structure, it has been investigated using a solid finite element model. Once defined the collapse behaviour of the simple structure, the analysis has been generalized using a concentrated plasticity finite element method. Results provided will be useful for studying generic reciprocal frame structures with several beams.

Keywords: reciprocal frame; nexorades; space structures; finite elements; collapse behaviour; temporary structures

1. Introduction

“Reciprocal Frame” is a structural system composed by bearing and supporting bars, used both for floor and roof (Chilton *et al.* 1995, Popovic *et al.* 1996, 1998). Thus a three-beams structure is the simplest reciprocal frame.

The first reciprocal frame structure appeared a long time ago. Chilton and Choo (1992) pointed out the impossibility to exactly define the origin of this particular structural system.

Japan is the native country of modern reciprocal frame architecture. Some evidences dates this structural system back to 12th century, when the Buddhist monk Chōgen (1121-1206) established a technique of spiral layering of wood beams which was used in building up temples and shrines. Chōgen’s technique is identical to the structural principles of modern reciprocal frame.

Throughout the centuries some famous architects and engineers such as Villard de Honnecourt in the Middle Ages (Erlande-Brandenburg *et al.* 1987), and Leonardo da Vinci and Sebastiano Serlio in the Renaissance (Popovic *et al.* 2008), dared to solve the problem of long-span roofs using short timber structural elements.

*Corresponding author, Assistant Professor, E-mail: sgambi@stru.polimi.it

^aAssociate Professor, E-mail: garava@stru.polimi.it

^bAssociate Professor, E-mail: attilio.pizzigoni@unibg.it

^cPh.D. Candidate

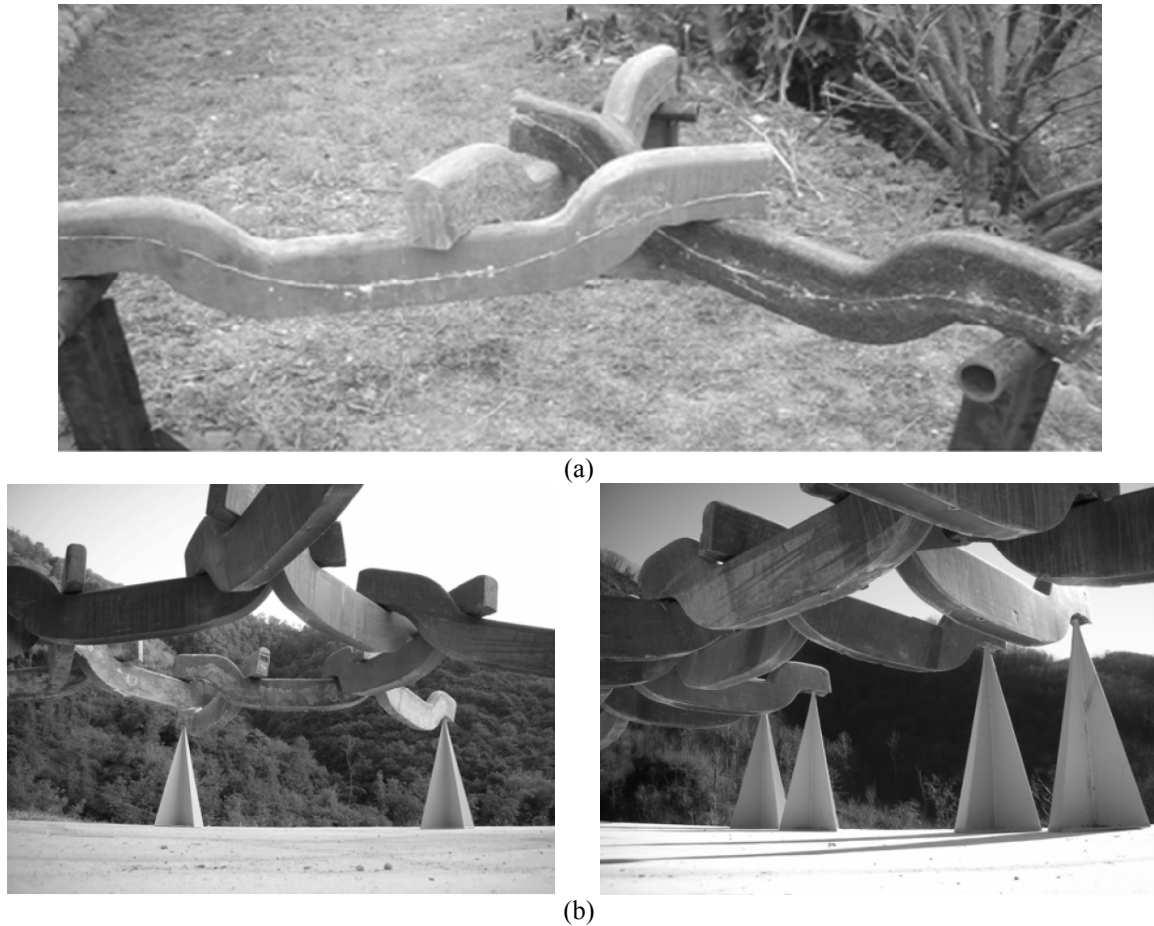


Fig. 1 Basic case-study reciprocal frame structure (a) and reciprocal frame structures with hexagon and square grid (b)

Combining various standard elements and joining them together result in both flat and three-dimensional structures. Thus a system turn to be a bi-dimensional planar surface but with a high bending strength which can be used for floor and ceiling construction.

For more than 260 years reciprocal frame system was neglected. Finally at the beginning of 1900 the Catalan architect Joseph Maria Jujol practically applied reciprocal frame principle to architecture (e.g., roof of Casa Negre, San Juan Despi, Barcelona, 1915; Casa Bofarul, Pallaresos, Tarragona, 1913-1918), and early in the 70's Wallis investigated the different planar morphologies of reciprocal grillages within a detailed study on the geometrical and mechanical principles of the load transfer of the structure (Wallis 1972). Wallis' contribution probably stirred up interest in studying and using reciprocal frame structures. Indeed, in the 90s Natterer *et al.* designed a 26-metre-span roof of a salt storage building at Lausanne in Switzerland (Popovic 2008). Another example using a similar structure is the about-7-metre diameter roof of a puppet theatre near Kumamoto, in Kyushu Island (Southern Japan) (Popovic 2008). More recently reciprocal frame technique has been used to design both gazebos and whisky barrelhouses in Scotland as well as

some buildings in Bradford (UK) (Popovic, 2008).

Actually, literature refers to reciprocal frame as “nexorades”. This name comes from the Latin word “nexor”, which means the basic cell-type structure. Baverel and Nooshin have investigated several nexorades based on regular polyhedral (2007). Rizzuto and Hulse have provided experimental and numerical modelling investigation on dodecahedral reciprocal space structures (2007). Douthe and Baverel introduced dynamic relaxation method to solve the form-finding problem in three-dimensional nexorades (2009). Kohlhammer has described the systemic behaviour of plane reciprocal frame structure; furthermore he has presented a general design and analysis method for practical usage (2011). In Gelez *et al.* (2012) a nexorade was used to build a prototype of an archaeological excavation shelter. Brocato and Mondardini have developed a FEM procedure for the design of stone domes based on Abeille’s bond (2012).

This paper approaches a nexorade analysis using a Finite Element Method. The study moves from a high performance-fibre-reinforced-concrete (Martinola *et al.* 2007) reciprocal frame temporary-system prototyped by Pizzigoni in 2008. Analytical and numerical investigations of collapse behaviour of a plane reciprocal frame structure made of fibre-reinforced concrete beams, shown in Fig. 1, have been developed.

Based on solid modelling, a finite element analysis has been performed and the ultimate strength and collapse mechanism have been pointed out. Then, using concentrated plasticity FE for beam, the analysis has been generalised and a nonlinear finite element analysis has been applied to larger structures. Finally, compared reciprocal frame systems with similar “traditional” structures, the analogy between their load capacity and collapse mechanism has come out.

Although reciprocal frame structures and traditional structures generally display similar collapse load conditions, the authors point out that considering structural safety, reciprocal frame systems are less robust. Given a serious local damage, the structural robustness defines the attitude of a system to survive to it without collapsing (Starossek and Haberland, 2011; Menchel *et al.*, 2011; Giuliani, 2012). There is a broad literature on structural robustness referred to the analysis of structures with a high social impact such as suspension bridges (Giuliani and Prisco, 2008), time-dependent structural behaviour for deteriorating systems (Biondini and Frangopol, 2010), multi-story frames subjected to dynamic load (Rezvani and Asgarian, 2012). Each beam involved in reciprocal frame structures is essential for ensuring the equilibrium of the beams next to it and the structural static stability. A local failure of a single beam causes the global collapse of the structure. Hence, even considering the philosophical view, reciprocal frame structures display an inherent poor robustness. Therefore a further research topic could concern the robustness enhancement.

2. The basic case study

Pizzigoni (2009) proposed a three-double s-beam modular case study. Hinges system joins beams together (Fig. 1(a)). As shown in Fig. 1(b), a different combination of these modular elements results in more complex structures and enables to build up plane reciprocal frame systems.

The beam’s cross-section is 6×14 cm, the full length of the beam is 1.2 m, with a distance between the two supports equal to 1 m. Those are very short beams and they are specially designed for both temporary narrow structures and structures leaning on every 3 or 4 meters. The narrow weight (about 250 N) enables to build more complex structures without using heavy lifting

Table 1 Mechanical and geometric properties

| Variable | Symbol | Value |
|------------------------|-----------------|-------------------------|
| Height | h | 14 cm |
| Width | b | 6 cm |
| Length | L | 100 cm |
| Young's Modulus | E | 58000 N/mm ² |
| Compression strength | f_c | 160 N/mm ² |
| Tension strength | f_t | 11 N/mm ² |
| Maximum tensile strain | ε_t | 0.003 |
| Beam weight | q | 0.23 kN/m |

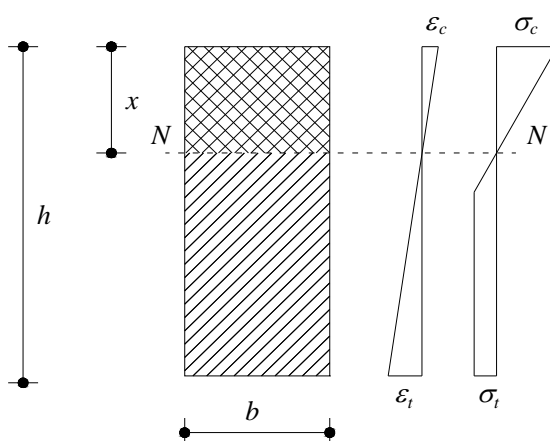


Fig. 2 Strain and stress outline over a beam cross-section

equipment. Furthermore the easy assembly enables to join beam to beam using a steel ball hinge.

Since beam design offers five different joint positions, some shape flexibility is provided. The leaning on the ground has been designed as a steel ball joint too. Thus since the beam can stay in the middle as well as at the ends of the structure, the beam-element's modularity is preserved.

3. Analytical evaluation

3.1 Collapse momentum assessment

Table 1 shows the mechanical and geometric properties of the beam-elements composing the reciprocal frame case-study.

The collapse behaviour analysis of the reciprocal frame case-study needs at first the ultimate moment assessment. Assuming that failure occurs when tensile strength is insufficient and compression degrees in the opposite fibres are well represented by a linear stress-strain diagram, the initial failure condition is shown in Fig. 2.

The neutral axis bisects the section and defines a compressed upper part and a stretched lower part. Thus both strain ε and stress σ in the outer tense fibre are known and they are defined by their ultimate value. Basing on translational equilibrium shown in linear stress-strain diagram of Fig. 2, the following equation comes out

$$\left(\frac{1}{2} \cdot E \cdot \varepsilon_t - f_t\right) \cdot x^2 + (2 \cdot f_t \cdot h) \cdot x - f_t \cdot h^2 = 0 \quad (1)$$

where E is Young's Modulus, and f_t is the material tensile strength. The solution x is the distance between the neutral axis and the cross-section compressed side. Basing on numerical data in Table 1, Eq. (1) has just one positive solution, $x = 37$ mm; this value corresponds to 63 MPa in maximum compressive stress, that is lower than the compressive failure of concrete, equal to 160 MPa. Thence the failure of the cross-section occurs in tensile area. Assessing rotational equilibrium over cross-sectional strengths at the failure time, the collapse moment is:

$$M_u = \frac{1}{2} \cdot b \cdot x \cdot \sigma_c \cdot \frac{2}{3} \cdot x + (h - x) \cdot b \cdot f_t \cdot \left(\frac{h - x}{2}\right) = 5.23 \text{ kNm} \quad (2)$$

3.2 Ultimate load assessment

Using the value of the collapse moment coming out of Eq. (2), the collapse load of the structure can be assessed. Fig. 3 represents the case-study geometry and the main substructure defining its static properties. This substructure has got a polar symmetry of 120° : the reciprocal supporting forces of each beam must obey the symmetry and they have the same strength.

Fig. 3 shows two types of loads and two types of constraint reaction forces acting on the structure: q is the beams dead load shown in Table 1 (0.23 kN/m) and P is an unknown additional load. Using analytical and numerical procedures the additional load has been evaluated. Applying this model, additional loads should act just on beams mutual supporting points. This hypothesis

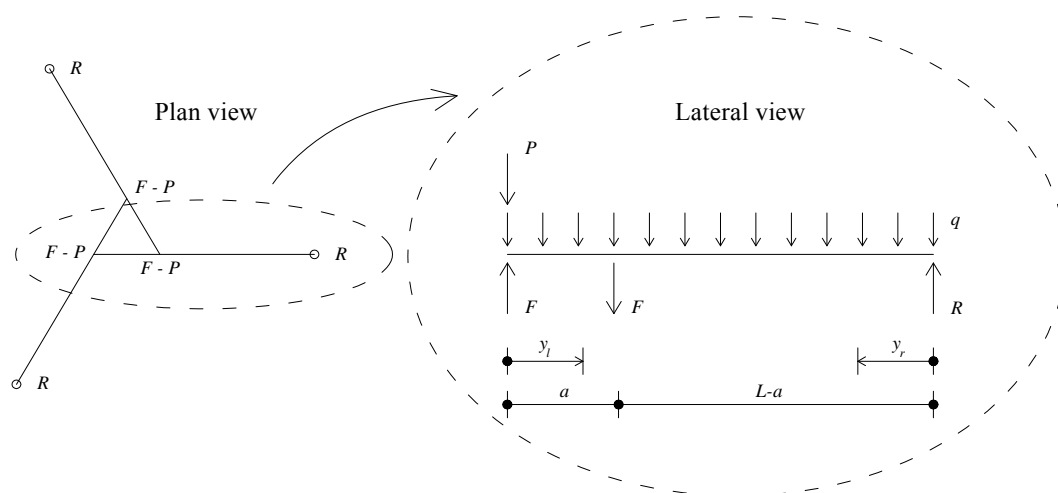


Fig. 3 Static outlines of the reciprocal frame case-study system and of one beam with mutual supporting forces F and joint reactions R

should stand to reason due to curved beams' narrow dimensions. On the right side, Fig. 3 shows a static outline with just one P -load acting on the mutual bearing points of the supported beam (see Fig. 1). While the constraint reaction R results from the fix constraint, the reaction F is the reciprocal supporting force.

Therefore it is enough considering just one of the three beams. Rotational equilibrium around the pinned joint provides

$$F = \frac{q \cdot L^2}{2 \cdot a} + \frac{P \cdot L}{2 \cdot a} \quad (3)$$

with uniformly distributed load q (structure dead load), local load applied on reciprocal supports P , distance between fix constraint and the furthest reciprocal support $L = 1$ m and distance between two reciprocal supports $a = 0.3$ m. The stability in vertical direction provides

$$R = q \cdot L + P \quad (4)$$

Based on the abovementioned relations (Eqs. 3 and 4), the bending momentum equation for the " $L - a$ " branch of beam on the left (M_l) is

$$M_l = (q \cdot L + P) \cdot y_l - \frac{q \cdot y_l^2}{2} \quad (5)$$

While the bending momentum equation for the " a " branch of beam on the right (M_r) is

$$M_r = \left[\frac{q \cdot L^2}{2 \cdot a} + \frac{P \cdot L}{2 \cdot a} - P \right] \cdot y_r - \frac{q \cdot y_r^2}{2} \quad (6)$$

Referring to a P -load higher than q -load, the cross-sectional area with the point load leads to the maximum bending moment (measuring in [m] and [kN])

$$M_l = (q \cdot L + P) \cdot y_l - \frac{q \cdot y_l^2}{2} = (q \cdot L + P) \cdot (L - a) - \frac{q \cdot (L - a)^2}{2} = 0.1046 + P \cdot 0.7 \quad (7)$$

Comparing the maximum bending moment with the ultimate strength (Eq. 2 and Eq. 7), the collapse load of the beam, P_b is

$$P_b = \frac{(5.23 - 0.1046)}{0.70} = 7.32 \text{ kN} \quad (8)$$

Since the structure has a polar symmetry, its collapse load is three times greater than the beam's collapse load. Thence the collapse load of the reciprocal structure P_s is assessed

$$P_s = 7.32 \cdot 3 = 22.0 \text{ kN} \quad (9)$$

Basing on collapse load the FEM analysis is performed.

4. Solid finite element model

A solid modelling of the reciprocal frame structure was performed in order to investigate the ultimate strength and eliminate any failure mechanism localized both in reciprocal supporting and

leaning parts. Using ABAQUS code, each beam of the structure has been modelled with solid tetrahedral elements with parabolic shape functions.

Considering material nonlinearity, the “damage plasticity” constitutive relation belonging to ABAQUS library is used (Lubliner *et al.* 1989, Lee and Fenves 1998, Sgambi *et al.* 2011a, Sgambi *et al.* 2011b). It is based on both plasticity and damage theory of concrete structures. The model assumes tensile cracking and compression fracture as the main failure modes. A penalty function method is used to model the contact nonlinearity. The whole model consists of 400000 degrees of freedom. The load condition is outlined as a set of compressive pressures over three small surface areas of the model (Fig. 4), with an increasing value up to the structure collapse.

In both reciprocal supporting and joint areas there is a steel ball joint. This joint assures rotational freedom of the system and an easy assembly of the structure at the same time. Using the real geometry and the material properties, inner and outer joints (steel ball joints) have been modelled. Thus the effective connection beam-to-beam can be considered and the potential occurrence of local failures due to steel balls influence can be numerically investigated. Introducing a steel ball joint in the supporting regions and rigidly joining it to the ground, the fix hinge joint have been modelled.

Hence, numerical model needs for two types of nonlinearity: material nonlinearity due to the fibre-reinforced concrete constitutive relationship and nonlinear contact due to the contact between beams and steel balls.

Numerical analysis provides a collapse load equal to 32.1 kN. This value is 46% higher than the ultimate load analytically evaluated. Probably the increase in collapse load is due to resisting mechanisms, ensued from finite element modelling and omitted in the simplified analytical model (Section 2). Fig. 5 shows the structural deformation and the plastic deformation occurred at the initial failure instant. Damage equally involves all the beams of the case study structure. The load displacement curve of one knot is shown in Fig. 6. There is an almost ductile behaviour related to tensile failure of fibre-reinforced concrete as well as an about 8-millimetre final displacement.

Fig. 7 represents in detail the pin joint’s vertical axis of symmetry cross-section of a beam both in deformed and non-deformed configuration. Note the element’s rotation around the steel ball joint.



Fig. 4 Numerical model perspective view. P forces representing additional load are located over the reciprocal bearing points (see Fig. 3)

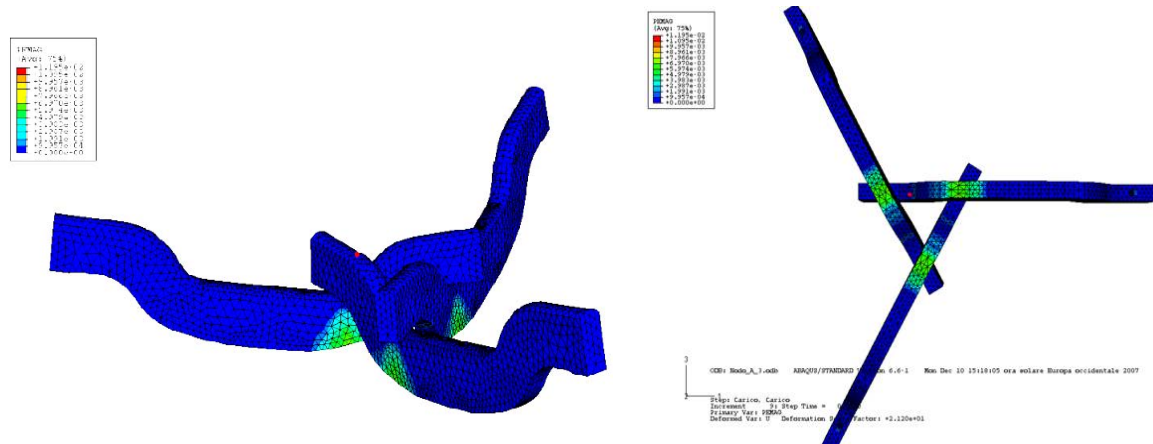


Fig. 5 Structural deformation and plastic deformation involving specific areas (perspective view on the left side, bottom-up view on the right side)

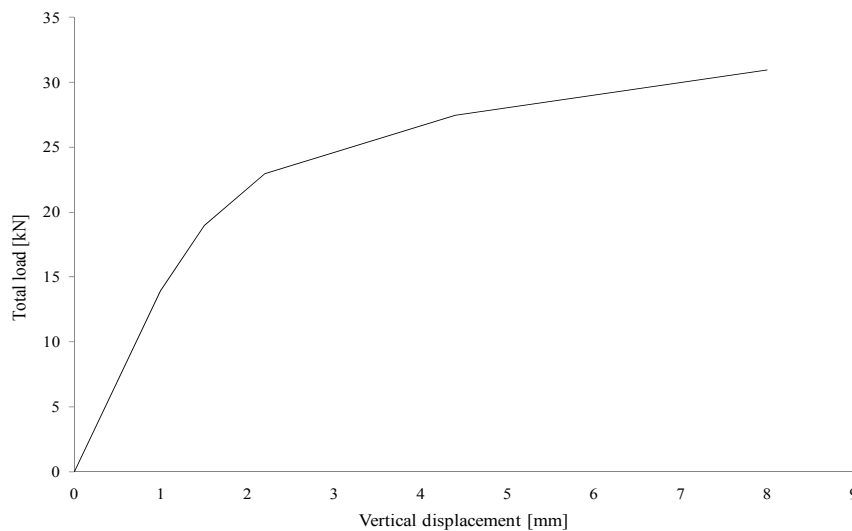


Fig. 6 Load-displacement curve describing the three-beam system model

Computation hasn't pointed out any failure localized close to the joints; furthermore considering mechanical characteristics of fibre-reinforced concrete, the steel ball joint's strengths result acceptable. The case-study analysis has pointed out a bending failure mechanism.

5. Concentrated plasticity model

5.1 Mechanical properties analysis of the concentrated plasticity model

Even if the FEAs performed are very detailed, their assessment becomes hard when they are performed over systems with more than three beams. Structural modelling technique and accuracy

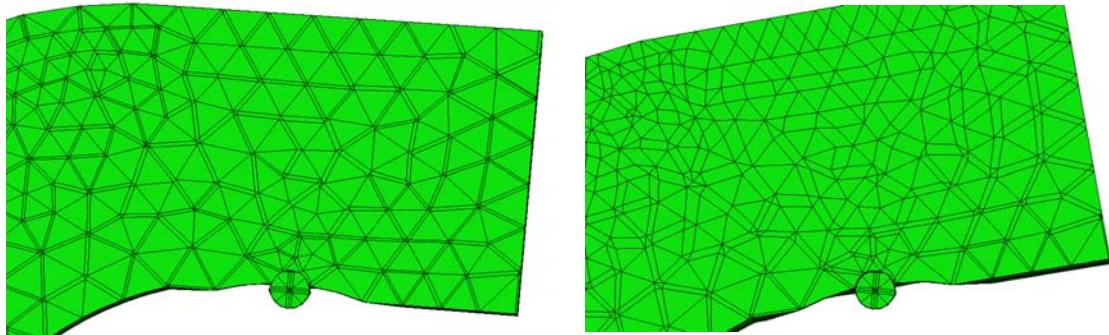


Fig. 7 Detailed outline of the beam's rotation around the steel ball end joint in non-deformed (upper) and deformed (lower) configuration

Table 2 Mechanical and geometric properties

| Moment [Nm] | Rotation |
|-------------|----------|
| 0 | -0.01 |
| 0 | -0.008 |
| -7900 | -0.008 |
| -5600 | 0 |
| 0 | 0 |
| 5600 | 0 |
| 7900 | 0.008 |
| 0 | 0.008 |
| 0 | 0.01 |

depends on the goal of its application (Sgambi *et al.* 2012). Referring to this case study, a solid modelling isn't a suitable method for evaluating the collapse behaviour of the system due to the high generalisation and cost. Therefore, basing on the results of preliminary analysis as well as FEAs for solid, the calibration of local nonlinear models (plastic hinge joint) with beam finite elements is set up. This modelling maintains the elements within the elastic field, while including plastic hinge joint leads to nonlinearity. Considering the nonlinear behaviour of the beam, the generic plastic hinge moment-rotation curve is defined (Table 2 and Fig. 8).

The moment-rotation relationship defining the nonlinear behaviour of the plastic hinge assumes that the hinge behaviour is linearly elastic by a bending moment threshold equal to 5600 Nm. No plastic rotation can take place between the sections. Then yield stress occurs and plastic rotation can arise up to 0.008 rad with a linearly increasing bending moment up to 7900 Nm. When this bending moment threshold is exceeded, failure due to excessive bending stress occurs. Both bending and rotational moments result from matching the load P -displacement curve of the concentrated plasticity model with the related curve of the FEM solid model introduced in the previous section (Fig. 6). The simplified analytic method describing the section behaviour has pinpointed a bending moment equal to 5230 Nm (Eq. 2) very close to the values provided by the comparison between the numerical models.

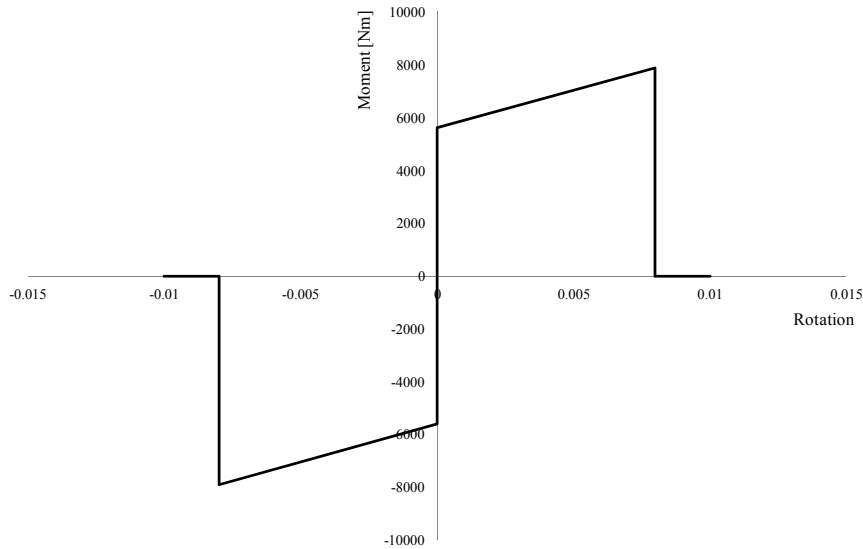


Fig. 8 Moment-rotation diagram of the case-study model

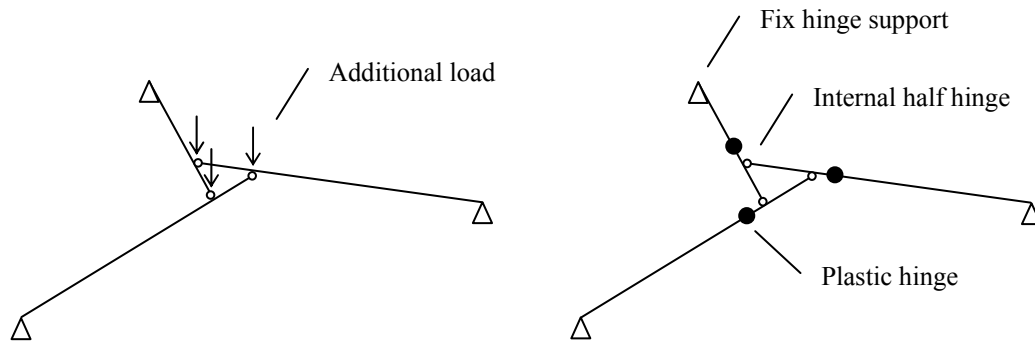


Fig. 9 Nonlinear model of the three-beam reciprocal frame case-study system (on the left side), plastic hinges final position (on the right side)

The geometric model of the three-beams structure is shown in Fig. 9. The model is composed by a typical finite element beam-model (two nodes each finite element and cubic shape functions) with nonlinear properties shown in Table 2. While at the outer end of each beam there is a fix hinge support, at the inner end an internal half hinge models the reciprocal support. Two types of loads act on the structure: the dead load (Table 2) and the three concentrated additional loads. Compared with the model described in the previous section, this is a simplified mechanical and geometric model. The three-dimensional computing provides a close-to-reality geometric model (Fig. 1 and Fig. 4).

The collapse of the system occurs when in the plastic hinges the plastic moment exceeds the value of 7900 Nm. Thus, one or more beams collapse and the structure is converted into a mechanism. Fig. 10 shows the load-displacement curve describing the analysis outcomes. The continuous curve represents the structural behaviour resulting from the concentrated plasticity

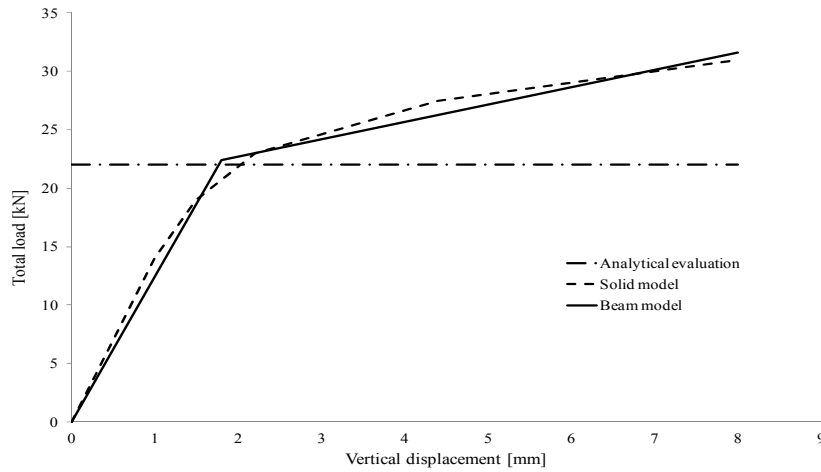


Fig. 10 Comparison between analytical evaluation, FEM solid model and beam model with local nonlinearity

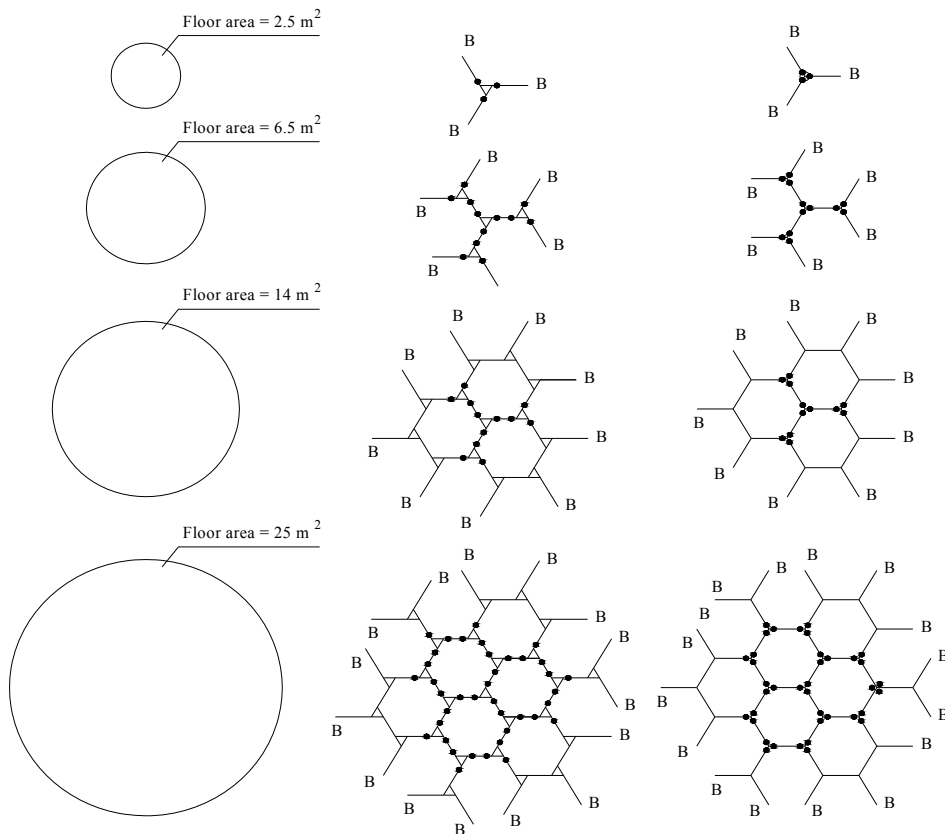


Fig. 11 Structural models involved in concentrated plasticity FE analyses: structures covered floor areas (on the left side), geometric models of the reciprocal frame structures (in the middle), and geometric models of the “traditional” structures (on the right side). Letter B indicates the fix constraint while the black dot indicates the plastic hinge position

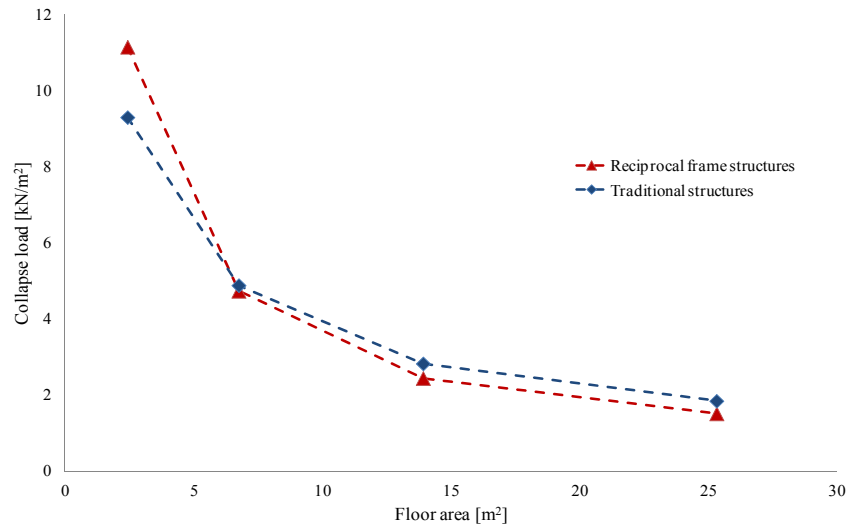


Fig. 11 Relation between live load variation and floor area variation

model; the dashes line describes the solid finite element modelling performed. Both the well posed approximation provided by FE beam model and the local nonlinearity result in a significant computational resources and time saving (few seconds versus some hours) providing a ultimate load very close to the one estimated by the FEA for solid model.

5.2 Generalised FEA applied to larger structures and comparison with “traditional” grids of beam

Considering all the cases in Fig. 11, a problem generalization was made. Fig. 11 shows three generalisation of the basic model previously described. Then 9, 24, and 45-beam-elements systems with respective covered floor area of 2.5 m² to 6.5 m², 14 m², and 25 m² (first column) have been investigated. The second column shows the geometry of the reciprocal frame structures. The third column shows the geometry of the similar “traditional” structures.

Based on the previously exposed approach, collapse analyses have been performed. Additional loads P act on the structure where the beams cross each other. Their values have been increased up to the structure collapse. Black dots represent plastic hinges positions when the collapse occurred. Fig. 11 shows that while the failures affected all the beams of the first two structures (plastic hinges have been formed in all the beams) the beams close to the edges of both the third and the fourth structures have remained in linear elastic region. In the latter cases plastic hinges have been formed in a central local area. Although there is a local damage, the whole structure has been affected by collapse.

The large number of plastic hinges shown in Fig. 11 is due to the constitutive relationship including hardening behaviour (Fig. 8). Indeed, the just formed plastic hinge was still able to withstand a bending moment increment and form further plastic hinges in other regions.

The structural collapse load has been evaluated for all the cases. The collapse load variation depending on the floor area covered has been finally investigated. Fig. 12 shows the values resulting from the analysis. The y-axis represents the collapse load per floor area (kN/m²), that is

the ratio between the sum of the concentrated loads acting on the model and the floor area covered by the structure. This approach has been applied for ensuring homogeneous results between different structures, and providing results related to existing standard service loads. Considering the smallest reciprocal frame structures here presented with collapse loads exceeding 5 kN/m^2 , they can be applied to temporary narrow-span floor; otherwise the largest ones with service loads from 2 to 3 kN/m^2 , can be applied to small roof systems.

The right column of the Fig. 10 and Fig. 11 show that the “traditional” structures analyses have provided similar results in terms of collapse loads and mechanisms. Slight differences in these values probably depend on slightly different structural geometries. Hence it is generally assumed that reciprocal frame structures and “traditional” structures show similar structural behaviours. The here presented structures can be effectively applied to temporary buildings with a great architectural impact.

6. Conclusions

Reciprocal frame architectures are effective and original design solutions with very old theoretical basis. Furthermore they propose to be innovative and optimal solutions for temporary roof with a great architectural impact due to their potential disassembly as well as their easily precast modular assembly. Considering structural behaviour analysis, optimization and reliability assessment, these systems investigation is still interesting.

Based on both analytical and numerical approach, this paper investigates a simple reciprocal frame structure made of three fibre-reinforced-concrete beams mutually supporting. Referring to analysis results performed on local nonlinear models, the parameters defining the plastic hinges behaviour have been conveniently arranged. Thus these models well represent ultimate load assessed by advanced solid FE model. The computational benefit enables to study more complex systems, extending the problem over wide span roof analysis.

Using this approach, 4 systems characterized by a reciprocal supporting and different span (3, 9, 24 and 45 beam-elements) have been investigated. Results point out the effectiveness of this particular structural typology in building removable flat ceiling with an about-10-square-metre narrow span. Wider structures are possible if there isn't an overload due to extra dead load. Similar analyses have been performed on traditional structures with the same geometry. Considering collapse loads and mechanisms, the analyses results pinpoint that reciprocal frame structures match similar traditional structures.

Further and future developments

Further and future research developments can concern materials and shape optimisation for a reliable application of reciprocal frame structures. Referring to structural safety, structural robustness of reciprocal frame structures should be improved. Using grid systems with redundant structural elements or designing more rigid mutual supporting nodes, the structural robustness of these particular structures can be enhanced. The potential disassembly as well as the easily assembly of these systems should be always ensured.

Acknowledgements

Authors are very grateful to Professor Paolo Riva and the engineer Luca Prandini for their helpfulness and invaluable suggestions over the study and the ABAQUS analysis. Furthermore authors wish to acknowledge the financial support of Italcementi Company.

References

- Baverel, O. and Nooshin, H. (2007), "Nexorades based on regular polyhedra", *Nexus Network Journal*, **9**(2), 281-298.
- Biondini, F. and Frangopol, D.M. (2010), "Structural robustness and redundancy of deteriorating concrete bridges", *Proceedings of the 5th International Conference on Bridge Maintenance, Safety and Management Philadelphia, USA, July*.
- Brocato, M. and Mondardini, L. (2012), "A new type of stone dome based on Abeille's bond", *International Journal of Solids and Structures*, **49**, 1786-1801.
- Chilton, J. and Choo, B.C. (1992), "Reciprocal frame long span structures", *Proceedings of the International Congress on Innovative Large Span Structures*, Montreal, Canada.
- Chilton, J., Choo, B.S. and Popovic, O. (1995), "Reciprocal Frames – Past, Present and Future", *Proceedings of Lightweight Structures in Civil Engineering*, Warsaw, Poland.
- Chilton, J., Choo, B.S. and Popovic, O. (1998), "The variety of reciprocal frame (RF) morphologies developed for medium span assembly building: a case study", *Journal of the International Association for Shell and Spatial Structures*, **39**(1), 29-35.
- Douthe, C. and Baverel, O. (2009), "Design of nexorades or reciprocal frame systems with the dynamic relaxation method", *Computers and Structures*, **87**, 1296-1307.
- Erlande-Brandenburg, A., Pernoud, R., Gimpel, J. and Bechmann, R. (1987), *Villard de Honnecourt*, Jaca Book, Milano.
- Gelez, S., Aubry, A. and Vaudeville, B. (2012), "Nexorade or Reciprocal Frame System Applied to the Design and Construction of a 850 m² Archaeological Shelter", *International Journal of Space Structures*, **26**(4), 303-312.
- Giuliani, L. (2012), "Structural safety in case of extreme actions", *International Journal of Lifecycle Performance Engineering*, **1**(1), 22-40.
- Giuliani, L. and Prisco, V. (2008), "Nonlinear analysis for progressive collapse investigation on reinforced concrete framed structures", *Proceedings Structures Congress 2008*, Vancouver, British Columbia, Canada.
- Kohlhammer, T. and Kotnik T. (2011), "Systemic behaviour of plane reciprocal frame structures", *Structural Engineering International*, **21**(1), 80-86.
- Lee, J. and Fenves, G.L. (1998), "Plastic-damage model for cyclic loading of concrete structures", *Journal of Engineering Mechanics*, **124**(8), 892-900.
- Lubliner, J., Oliver, J., Oller, S. and Oñate, E. (1989), "A plastic-damage model for concrete", *International Journal of Solids and Structures*, **25**, 299-329.
- Menchel, K., Massart, T.J. and Bouillard, Ph. (2011), "Identification of progressive collapse pushover based on a kinetic energy criterion", *Structural Engineering and Mechanics*, **39**(3), 427-447.
- Martinola, G., Meda, A., Plizzari, G.A. and Rinaldi, Z. (2007), "Strengthening of R/C beams with high performance fiber reinforced cementitious composites", *Proceedings of HPFRCC 5 - High Performance Fiber Reinforced Cement Composites*, Mainz, Germany.
- Pizzigoni, A. (2009), "A high fiber reinforced concrete prototype for reciprocal structures of demountable building", *Proceedings of the IASS Symposium 2009*, Valencia, Spain.
- Pizzigoni, A. and Sgambi, L. (2008), "Comportamento meccanico di strutture spaziali reciproche". *Proceedings of the Handling Exceptions in Structural Engineering Congress*, Roma, November. (in Italian)

- Popovic, O. (2008), *Reciprocal Frame Architecture*, Architectural Press, Elsevier, Slovenia.
- Popovic, O., Chilton, J.C. and Choo, B.S. (1998), "The variety of reciprocal frame morphologies developed for a medium span assembly building", *Journal of the Association for Shell and Space Structures*, **39**(1), 29-35.
- Popovic, O., Chilton, J.C. and Choo, B.S. (1996), "Rapid construction of modular buildings using the 'reciprocal frame'", *Proceedings of the International Conference on Mobile and Rapidly Assembled Structures*, Seville, Spain, June.
- Rezvani, F.H. and Asgarian, B. (2012), "Element loss analysis of concentrically braced Frames considering structural performance criteria", *Steel and Composite Structures*, **12**(3), 231-248.
- Rizzuto, J. and Hulse, R. (2007), "Dodecahedric mutually supported element space structure: experimental Investigation", *International Journal of Space Structures*, **22**(2), 107-121.
- Sgambi, L., Gkoumas, K. and Bontempi, F. (2012), "Genetic algorithms for the dependability assurance in the design of a long-span suspension bridge", *Comp.-Aided Civil and Infrastruct. Engineering*, **27**(9), 655-675.
- Sgambi, L., Oلماتي, P., Petrini, F. and Bontempi, F. (2011A), "Seismic performance assessment of precast element connections", *Proceedings of 2011 PCI Annual Convention and National Bridge Conference*, Salt Lake City, UT 84101, USA.
- Sgambi, L., Zambelli, S., Pagani, C. and Bontempi, F. (2011B), "Experimental and numerical assessment of a special joint connection for precast columns", *Proceedings of the 2011 World Congress on Advances in Structural Engineering and Mechanics*, Seoul, Korea.
- Starossek, U. and Haberland, M. (2011), "Approaches to measures of structural robustness", *Structure and Infrastructure Engineering*, 7(7-8), 625-631.
- Wallis, J. (1972), *Opera Mathematica*, Goerg Olms Verlag Hildesheim, New York.